

FIG 1 Circular representation of pBSC2-1 (A) and pBSC2-2 (B). Features depicted by the circles from outside (1) to inside (5) are as follows: circle 1, scale marked in 5-kb intervals; circle 2, ORFs present in the reverse strand; circle 3, ORFs present in the forward strand; circle 4, G+C content (sea green and magenta indicate values greater than and less than the average G+C content, respectively); circle 5, G+C skew bias ($[G - C]/[G + C]$) (red indicates values below average and blue indicates values above average). ORFs are colored according to their function: red, plasmid replication and maintenance; orange, conjugation; light green, ORFs having homology to some functional proteins; dark green, nitrogen metabolism; blue, transposase-like proteins; light gray, hypothetical proteins; dark gray, conserved hypothetical proteins. The singleton *pmoC* (marked with an arrow) and its upstream regulatory gene in pBSC2-2 are colored sky blue.

Plasmid curing. Attempts to cure the plasmids by using ethidium bromide or acridine orange were made. Prior to curing, the sublethal concentrations of the curing agents were determined for strain SC2. At 30°C, these were around 100 $\mu\text{g ml}^{-1}$ and 200 $\mu\text{g ml}^{-1}$ for ethidium bromide and acridine orange, respectively. Cells were grown with the above concentrations of DNA-intercalating agents (initial optical density at 600 nm $[\text{OD}_{600}]$ of 0.04) for 15 days. Cell broth was then suitably diluted and spread on AMS agar plates and incubated. Similar trials were also done at 37°C. However, due to very poor growth, the plates were not analyzed further. Single colonies that appeared on plates incubated at 30°C were randomly selected (100 colonies for each treatment) and checked for loss of plasmids by PCR using the same primers as used for probe generation in Southern hybridization (see Table S1 in the supplemental material). For colony PCR, cells were lysed using Lyse and Go PCR reagent (Thermo Scientific, Rockford, IL). The cell lysates contained both genomic and plasmid DNA templates.

Sequencing strategy and assembly. Two plasmid sequences were assembled from a whole-genome shotgun project for *Methylocystis* sp. strain SC2. Whole-genome shotgun data were obtained by pyrosequencing using the GS FLX Titanium platform (454 Life Sciences, Branford, CT). In addition, a fosmid library with 37-kb inserts (CopyControl fosmid library production kit; Epicentre, Madison, WI) was constructed. End sequencing of 4,000 fosmid inserts was performed using BigDye 3.1 chemistry and 3730XL capillary sequencers (ABI, Darmstadt, Germany). Sequence reads obtained from 454 and Sanger sequencing were assembled by the MIRA assembler (13). A preliminary data analysis indicated the presence of two plasmids in strain SC2. Corresponding contigs were finished by primer walking and manually curated in Consed (17). The obtained plasmid sequences for pBSC2-1 and pBSC2-2 show sequencing coverages of 52- and 56-fold, respectively, on average. The potential open reading frames (ORFs) were established with GLIMMER 2.1 (15). The predicted ORFs and putative intergenic sequences were further examined manually using the Artemis platform (6). BLAST searches (1) against the NCBI nonredundant protein database and Swiss-Prot protein database were per-

formed to determine the ORFs. Circular plasmid maps were drawn using DNA plotter (7). The deduced amino acid sequences of the *pmoC* product were aligned in MEGA (v4.0.2) using CLUSTALW, and a phylogenetic tree was constructed using the *p*-distance matrix of neighbor-joining algorithms. Bootstrap analyses were performed with 1,000 replications. Similar tree topologies were obtained with neighbor-joining and maximum-likelihood methods.

Nucleotide sequence accession numbers. The complete sequences of pBSC2-1 and pBSC2-2 have been deposited in the EMBL, GenBank, and DDBJ databases under the accession numbers FO000001 and FO000002, respectively.

RESULTS AND DISCUSSION

Two large, low-copy-number plasmids are present in strain SC2. Complete nucleotide sequences of two novel plasmids were obtained during assembly of the genome sequence of strain SC2 and were found to be of 229.6 kb (pBSC2-1) and 143.5 kb (pBSC2-2) with average G+C contents of 60.7 and 60.4 mol%, respectively (Fig. 1). Sequences of both plasmids were obtained together with the genome sequence from a whole-genome shotgun approach. This allowed us to estimate the copy numbers of the plasmids by comparing their average sequence coverages (27). As pBSC2-1 and pBSC2-2 were obtained with sequence coverages (52- and 56-fold, respectively) similar to that of the chromosome (53-fold), we assume that the plasmids are present in single copy. PFGE followed by Southern blot analysis clearly showed the presence of two bands corresponding to the expected sizes (based on sequence assembly) of the plasmids, in addition to the genome (Fig. 2). Distinct bands representing the two plasmids were always detected in PFGE, regardless of whether log- or stationary-phase cells (Fig. 2) or cells grown at different methane concentrations (0.2% and 20% methane; data not shown) were analyzed. The

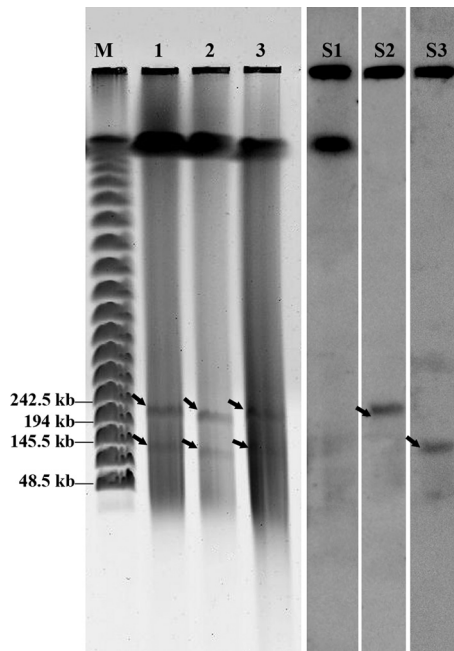


FIG 2 PFGE followed by Southern hybridization shows the presence of two plasmids in strain SC2. Lane M shows Lambda PFG marker (New England BioLabs, Ipswich, MA) containing successively larger concatemers of lambda DNA, with sizes of representative bands shown on the left. Lanes 1 and 2 contain plugs of strain SC2 cells harvested in log phase and stationary phase, respectively. Lane 3 contains a plug of strain SC2 cells harvested in log phase followed by S1 nuclease treatment. The two plasmids are marked by arrows. The plasmids showed similar migration patterns, regardless of whether or not SC2 cells had been treated with S1 nuclease. Therefore, Southern hybridization results are shown only for the electrophoresis pattern in lane 1, using probes specific to genomic DNA (lane S1), pBSC2-1 (lane S2), and pBSC2-2 (lane S3).

banding patterns in PFGE and Southern hybridization from S1 nuclease-treated and untreated plugs were similar. These results strongly support the independent existence of two plasmids in strain SC2, ruling out the rare possibility that the assembled contigs are integrative conjugative elements or mobile excisable elements.

Of the 240 and 152 predicted ORFs in pBSC2-1 and pBSC2-2, respectively, 121 (50%) and 72 (47%) were assigned putative functions, 58 (24%) and 25 (16%) encoded conserved hypothetical proteins, and 28 (12%) and 23 (15%) ORFs were putative novel. Moreover, 33 (14%) ORFs in pBSC2-1 and 32 (21%) in pBSC2-2 encode transposase-like proteins, thereby suggesting possible DNA rearrangement events in both plasmids. The ORFs present in the two plasmids and their annotations are described in Tables S2 and S3 in the supplemental material. For the unique ORF identifiers, P1 or P2 refers to the respective plasmid pBSC2-1 or pBSC2-2, and the subsequent number corresponds to the ORF number.

The plasmids contain a *repABC* replication module. Dot plot analysis showed that the two plasmids share only a few conserved regions (see Fig. S1 in the supplemental material), in particular, the replication module consisting of *repABC* genes (P1_12 to P1_14 and P2_74 to P2_76). The *repABC* family of replicons is reported to be present in large, low-copy-number plasmids and on some secondary chromosomes in at least 19 alphaproteobacterial genera, mainly belonging to the *Rhizobiales*, *Rhodobacterales*,

and *Rhodospirillales* (8, 10). It has also been reported that more than one plasmid replicating via the *repABC* module can coexist in a single organism (25). The replicon consists of three clustered genes (*repA*, *repB*, and *repC*) that are transcribed in the same direction. The first two genes are involved in partition with the partition site (*parS*) located at different positions throughout the replicon in different plasmids (10). The third gene, *repC*, is involved in replication, with the replication origin present in an AT-rich stretch of the gene itself (9, 10). A short, AT-rich, highly conserved intergenic sequence (*igs*) is located between *repB* and *repC* (9, 10). From the *igs* region, a small nontranslated antisense RNA (ctRNA) is transcribed in the direction opposite that of *repABC*. The ctRNA is found in all *repABC* operons and controls replication of the plasmid (10, 11). We could identify complete *repABC* replication modules in both plasmids having all essential features, including the conserved *igs* region and the consensus promoter sequence for the ctRNA (Fig. 3). A putative *parS*-like consensus sequence was also identified within *repB* in both plasmids (Fig. 3). In addition, several copies of genes encoding single-strand binding proteins were identified in both of them (P1_149, P1_180, P1_186, P1_192, P2_1, and P2_21).

Eighty-eight ORFs (37%) in pBSC2-1 and 28 ORFs (18%) in pBSC2-2 showed maximum homology in BLASTX searches with proteins encoded by the genome of *Methylocystis* sp. strain Rockwell. When similar BLAST searches were done with remaining ORFs from both plasmids, proteins encoded by the genomes of *Methylocystis* sp. strain Rockwell and/or *Ms. trichosporium* OB3b appeared in the first five hits in most of them. This indicates that almost all plasmid-carried ORFs in strain SC2 are present in both strain Rockwell and strain OB3b. This, however, does not prove that the two latter strains contain similar plasmids, as the homologous ORFs were found scattered across different contigs of the released genome sequences and the regions of homology were never in reasonably large contigs. Interestingly, we could identify the alphaproteobacterial plasmid-specific replication module in both draft genomes. While *Methylocystis* sp. strain Rockwell was found to contain the genes in three distinct contigs (ctg177 [NZ_AEVM01000027], ctg148 [NZ_AEVM01000047], and ctg161 [NZ_AEVM01000028]), they were detected in two different contigs in *Ms. trichosporium* OB3b (ctg00105 [NZ_ADVE01000033] and ctg00122 [NZ_ADVE01000105]). The presence of these multiple *repABC* operon copies in the genome sequences of *Methylocystis* sp. strain Rockwell and *Ms. trichosporium* OB3b strongly supports the existence of plasmids, which is further corroborated by previous studies that reported the occurrence of plasmids in *Methylocystis* spp. and *Ms. trichosporium* OB3b (24). Thus, after whole-genome gap closure, such plasmids may be identified as separate entities in strains Rockwell and OB3b. However, we could not identify the *repABC* genes in the recently released plasmid sequence of *Mm. alcaliphilum* strain 20Z, which might propagate via some different method. The absence of the *repABC* genes appears logical, as *Mm. alcaliphilum* is a member of the *Gammaproteobacteria*.

Additional plasmid-related features of pBSC2-1 and pBSC2-2. Apart from the *repAB* genes, which provide a partition function, additional loci that could ensure the faithful segregation of the two plasmids to daughter cells were identified. In pBSC2-2, a *parAB* locus (P2_23 to P2_24) was identified. These genes could encode a ParA-like ATPase and a ParB-like partition protein. pBSC2-1 was found to encode a RelBE family toxin-antitoxin system (P1_206 to P1_207), which is commonly present on large

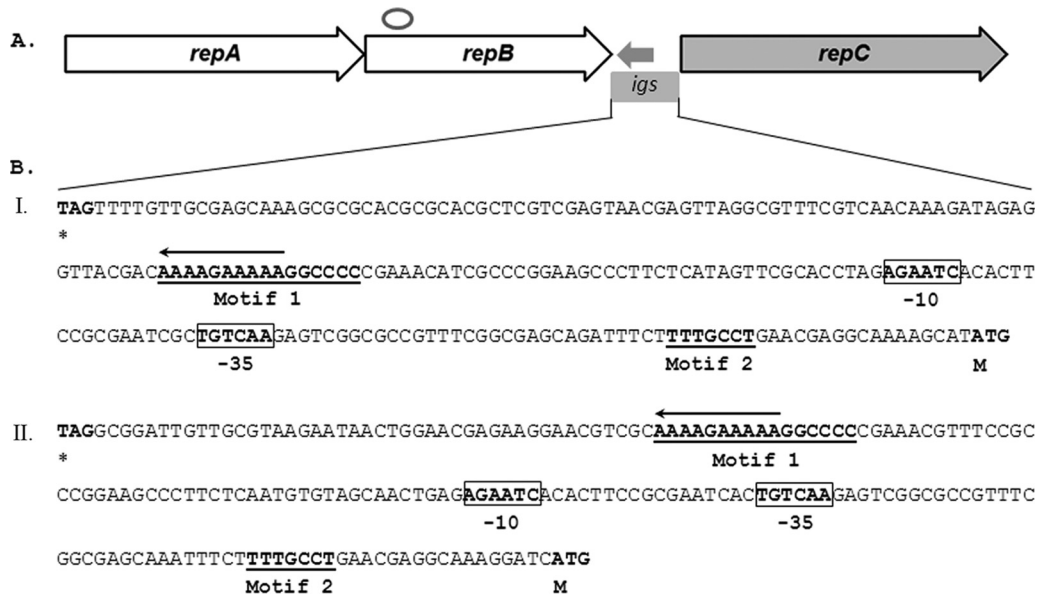


FIG 3 Schematic representation of the *repABC* replication module in pBSC2-1 and pBSC2-2. (A) Open arrows (*repA* and *repB*) and the filled arrow (*repC*) indicate *repABC*, with the arrowheads showing their transcription directions. The small arrow in the opposite direction between *repB* and *repC* indicates the position of the putative antisense RNA (ctRNA). The position of the putative *parS* site is marked as an open circle. In both plasmids, a *parS*-like consensus sequence (GTTNNCNGCNGNNAAC) (10) is present within *repB*. The conserved intergenic region (*igs*) between *repB* and *repC* is marked by a box. (B) Nucleotide sequences of the intergenic region (*igs*) in pBSC2-1 (I) and pBSC2-2 (II). In both cases, sequences are shown from the stop codon of *repC* to the start codon of *repC* (both highlighted by boldface letters and indicated below by the respective codes, * and M). The -35 and -10 elements of the ctRNA promoter are indicated, boldface and boxed. The motifs 1 and 2, indicated in boldface and underlined, are conserved in the *igs* of *repABC* replicons. The T-tract, which probably constitutes the end of the transcript, is marked by an arrow, with an arrowhead showing the direction of transcription.

plasmids and chromosomes. The toxin component (RelE) represses translation, probably by binding to ribosomes, and the antidote protein (RelB, a member of the Arc/MetJ repressor family) stably binds and deactivates the toxin (26). A complete type IV secretion system locus (*avhB1* [*virB1*] to *avhB11* [*virB11*]) was identified in both plasmids (P1_220 to P1_230 and P2_39 to P2_50), followed by *traG* in pBSC2-1 (P1_219) and *virD4* in pBSC2-2 (P2_38) (Fig. 1; see also Tables S2 and S3 in the supplemental material). In plasmids like RP4, Ti, and pBTK445, it has been shown by mutational analysis that their *avhB* (*virB*) loci are involved in the conjugative transfer function (14, 18). Thus, both pBSC2-1 and pBSC2-2 might also have a conjugative transfer function.

During PCR-based screening for the loss of plasmids, all colonies obtained after treatment with the DNA-intercalating agents (ethidium bromide and acridine orange) tested positive for both the plasmids and the genome. Thus, the plasmids were not cured by either of the DNA-intercalating agents. This may be accounted to the segregation mechanisms encoded by pBSC2-1 and pBSC2-2, which confer high plasmid stability. The incapability of plasmid curing by DNA-intercalating agents is quite often observed for similar large, low-copy-number plasmids (14, 37).

ORFs with significant similarity to metabolically important genes. Mercury resistance (*mer*) genes were identified in both plasmids. While only *merR* and *merT* were identified in pBSC2-2 (P2_70 to P2_71), a *mer* operon, constituting the essential genes *merR*, *merT*, *merP*, and *merA* (P1_153 to P1_156), was identified in pBSC2-1. The characterized *mer* operons from different bacteria vary in structure and are generally composed of genes that encode the functional proteins for regulation (*merR*), trans-

port (*merT*, *merP*, and/or *merC*), and reduction (*merA*) (3, 35). Several functional *mer* operons from *Proteobacteria* have been reported to contain the minimum number of genes. These include *merRTPAD* and *merRTPCAD*, carried by Tn501 and Tn21, respectively (3, 19). While the former operon does not contain a *merC*, the one present in the latter was shown by mutational analysis to have no effect on mercury resistance (19). Moreover, the *merD* gene, which is present in both operons, encodes an additional regulatory component. Its deletion does not hamper the mercury resistance phenotype (3). Based on these findings, we anticipated that the *mer* operon carried by pBSC2-1 might be functional and could provide resistance to only inorganic mercurial compounds (narrow spectrum), as it lacks *merB*, which together with *merA* confers resistance to organomercuric compounds (35). When grown on AMS plates supplemented with various concentrations of HgCl₂, strain SC2 could resist only up to 0.1 μg ml⁻¹ of HgCl₂. This is at least 10- to 100-fold less than in other bacteria that harbor well-characterized mercury resistance plasmids (19). Some other heavy metal resistance genes were also identified in pBSC2-1, and these included three sets of genes encoding a heavy metal efflux pump belonging to CzcA family and an upstream efflux transporter belonging to the RND family (P1_88 to P1_90, P1_124 to P1_127, and P1_174 to P1_175). The presence of heavy metal resistance genes could be due to the fact that strain SC2 was isolated from a highly polluted aquifer in Germany (16). In addition, several copper transport-related genes were identified in pBSC2-1. These include multiple copies of genes encoding either the copper-binding protein CusF (P1_123, P1_130, and P1_167) or a CtpA-like copper-transporting P-type ATPase (P1_50, P1_55, P1_120, and P1_121). This transporter is

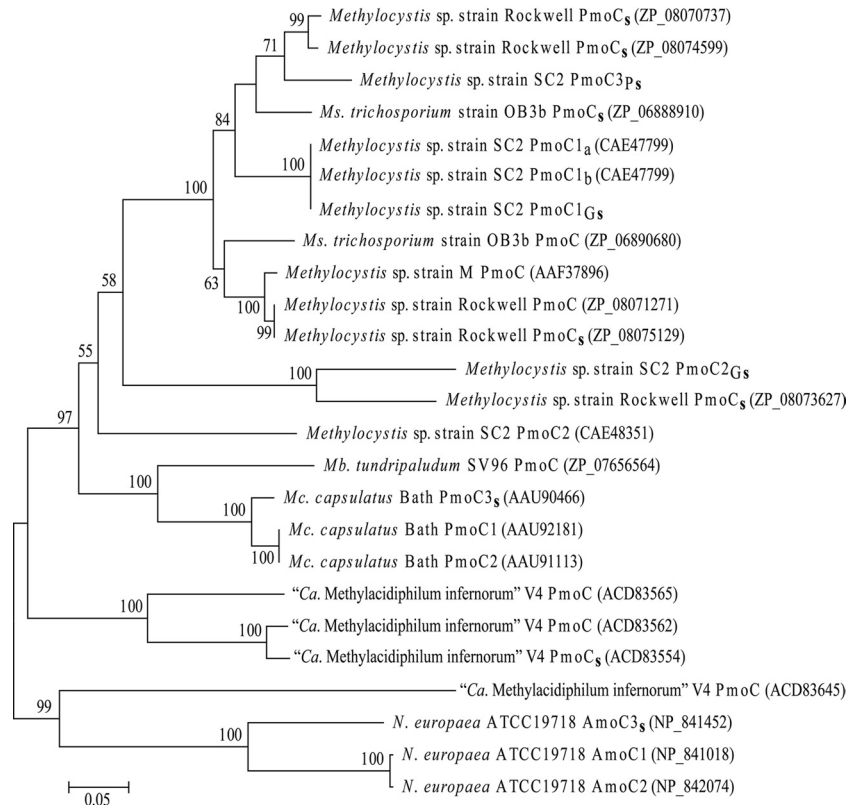


FIG 4 Neighbor-joining tree showing the phylogenetic analysis of the derived amino acid sequences encoded by *pmoC*. The amino acid sequences of PmoC used in the tree construction were deduced from the singleton copies and *pmoCAB* operons present in the genomes of *Mc. capsulatus* Bath, *Mb. tundripaludum* SV96, *Ms. trichosporium* OB3b, *Methylocystis* sp. strain Rockwell, *Methylocystis* sp. strain SC2, *Methylocystis* sp. strain M, and "Ca. Methylocidiphilum inferorum" V4. The accession numbers of the respective PmoC proteins are given in parentheses. Singleton *pmoC* copies of all the methanotroph strains are marked with "s" in their designations. Singletons from strain SC2 are labeled with "G" or "P" to distinguish between the genome- and plasmid-carried copies. AmoC sequences from *Nitrosomonas europaea* ATCC 19718 (NC_004757) were also included. Bootstrap values above 50 are shown. The scale bar represents 0.05 substitutions per amino acid position.

known to supply copper to membrane-associated proteins that require this metal as a cofactor (20). The presence of copper transport genes in the plasmid is interesting, as several enzymes, including the primary metabolic enzyme (pMMO), are copper dependent (29).

Both plasmids also carry genes that generally encode proteins with housekeeping functions. In pBSC2-2, these include genes that encode a DNA-directed DNA polymerase (P2_29) and the sigma factor of RNA polymerase (P2_6 and P2_117). pBSC2-1 encodes subunits of the F_oF₁-ATP synthase complex (P1_97 to P1_105). It also contains genes encoding key enzymes of glycolysis, namely, phosphofruktokinase (P1_63), phosphoenolpyruvate synthase (P1_64, P1_145, and P1_151), and glyceraldehyde-3-phosphate dehydrogenase (P1_66). Interestingly, all these ORFs are surrounded by transposase-like proteins, suggesting possible genomic rearrangement or duplication events, as all these genes are also present in the genome of strain SC2.

A nitric oxide reductase gene was identified in both plasmids (P1_45 and P2_130). In addition, a complete *nos* operon (*nosRZDFYX*) (P2_139 to P2_144) for nitrous oxide reductase was identified in pBSC2-2 (21, 28). Genes encoding a hybrid cluster protein (hydroxylamine reductase) (P2_147 and P2_148) was found adjacent to the *nos* operon, suggesting operation of a pathway for hydroxylamine detoxification by reduction to ammonium (32, 33). Methanotrophs are known to

produce nitrite and nitrous oxide during growth on methane, apparently due to aerobic oxidation of ammonia and hydroxylamine (32). The genes for nitrification and denitrification are widespread in methanotrophs, and the encoded enzymes show functional redundancy. However, the genes for nitrous oxide reductase have not been detected in any of the genome-sequenced methanotrophs (32). Thus, the presence of a complete plasmid-borne *nos* operon in strain SC2 is unique among genome-sequenced methanotrophs and might enable SC2 cells to convert the greenhouse gas nitrous oxide to dinitrogen. A functional *nos* operon has been detected earlier on the megaplasmid pSymA of the symbiotic nitrogen-fixing soil bacterium *Sinorhizobium meliloti* (21).

A singleton *pmoC* is present in pBSC2-2. An interesting feature is the presence of a singleton *pmoC* (*pmoC3_{p_s}*) in pBSC2-2 (P2_56), which could encode the PmoC subunit of pMMO. Five additional copies of *pmoC* were identified in the genome of strain SC2, including three as part of the *pmoCAB* gene clusters (*pmoC1_a*, *pmoC1_b* and *pmoC2*) encoding pMMO isozymes (2) and two singletons (*pmoC1_{G_s}* and *pmoC2_{G_s}*; unpublished data). The amino acid sequence deduced from the plasmid-borne *pmoC* (PmoC3_{p_s}) showed greatest homology (88%) to the conventional PmoC1_a and PmoC1_b and contains the conserved Asp129, His133, and His146 residues. These three residues are present in all well-characterized PmoC proteins and are involved in the coordination of copper along with Glu200 of PmoA in the mononu-

clear copper-binding site of pMMO (30). Isolated copies of *pmoC* have been repeatedly found in type I and type II methanotrophs, and these include four copies in *Methylocystis* sp. strain Rockwell (31) and one copy each in *Mc. capsulatus* Bath (39) and *Ms. trichosporium* OB3b (33). One singleton *pmoC* was identified even in the distantly related “*Ca. Methylophilum inferorum*” V4 genome (22). To determine the evolutionary origin of the plasmid-borne *pmoC*, a tree was constructed by using the amino acid sequences deduced from all the singleton *pmoC* genes reported above and representatives from the *pmoCAB* operons. PmoC_{3Ps} showed a clear affinity to two *pmoC* singletons of *Methylocystis* sp. strain Rockwell and the lone copy from *Ms. trichosporium* OB3b (Fig. 4). A transcriptional regulator (P2_55) containing an N-terminal amidase domain and a C-terminal AraC-type DNA-binding helix-turn-helix (HTH) domain was identified upstream of *pmoC*_{3Ps} and the two singletons in strain Rockwell. In *Ms. trichosporium* OB3b, the upstream transcriptional regulator belongs to the LysR family. Conclusive results on the functional role of the singleton *pmoC* copies are not yet available for any methanotrophic bacterium. Attempts to generate *pmoC3* chromosomal insertion null mutants in *Mc. capsulatus* Bath were made but were unsuccessful. Therefore, Stolyar et al. suggested that *pmoC3* may play an essential role in growth on methane (34). Our attempts to generate knockout mutants of singleton *pmoC* genes, whether present in the genome or present in the plasmid, also failed. Information on the methods used to achieve *pmoC* knockout mutants is given in the supplemental material (supplemental methods and Fig. S2). After the second recombination, no in-frame deletions were obtained and all tested clones were wild-type revertants. This may suggest that, like *pmoC3* in *Mc. capsulatus* Bath, all three singleton *pmoC* genes present in strain SC2, including the plasmid-borne one, are essential for methanotrophic growth.

In conclusion, strain SC2 was found to harbor two novel *repABC*-containing plasmids that are stably maintained due to the presence of dual partition systems and could be conjugative in nature. They also contain genes related to the methanotrophic mode of life. While one carries a singleton *pmoC*, the other has genes related to copper transport, which is indirectly related to proper functioning of pMMO. Further characterization of genes present in pBSC2-1 and pBSC2-2 will provide insights into the functional role these plasmids are playing in methanotrophs.

ACKNOWLEDGMENTS

This project was funded by the LOEWE Research Center for Synthetic Microbiology (SYNMIKRO) and the Max Planck Society. B.D. is grateful to the Alexander von Humboldt Foundation for his fellowship. S.D. is a postdoctoral fellow of the Max Planck Society.

We thank Klaas Schotanus for his help running PFGE.

REFERENCES

- Altschul SF, et al. 1997. Gapped BLAST and PSI-BLAST: a new generation of protein database search programs. *Nucleic Acids Res.* 25:3389–3402.
- Baani M, Liesack W. 2008. Two isozymes of particulate methane monooxygenase with different methane oxidation kinetics are found in *Methylocystis* sp. strain SC2. *Proc. Natl. Acad. Sci. U. S. A.* 105:10203–10208.
- Barkay T, Miller SM, Summers AO. 2003. Bacterial mercury resistance from atoms to ecosystems. *FEMS Microbiol. Rev.* 27:355–384.
- Barton BM, Harding GP, Zuccarelli AJ. 1995. A general method for detecting and sizing large plasmids. *Anal. Biochem.* 226:235–240.
- Boden R, et al. 2011. Complete genome sequence of the aerobic marine methanotroph *Methylomonas methanica* MC09. *J. Bacteriol.* 193:7001–7002.
- Carver T, et al. 2008. Artemis and ACT: viewing, annotating and comparing sequences stored in a relational database. *Bioinformatics* 24:2672–2676.
- Carver T, Thomson N, Bleasby A, Berriman M, Parkhill J. 2009. DNAPlotter: circular and linear interactive genome visualization. *Bioinformatics* 25:119–120.
- Castillo-Ramirez S, Vazquez-Castellanos JF, Gonzalez V, Cevallos MA. 2009. Horizontal gene transfer and diverse functional constraints within a common replication-partitioning system in *Alphaproteobacteria*: the *repABC* operon. *BMC Genomics* 10:536. doi:10.1186/1471-2164-10-536.
- Cervantes-Rivera R, Pedraza-Lopez F, Perez-Segura G, Cevallos MA. 2011. The replication origin of a *repABC* plasmid. *BMC Microbiol.* 11:158. doi:10.1186/1471-2180-11-158.
- Cevallos MA, Cervantes-Rivera R, Gutierrez-Rios RM. 2008. The *repABC* plasmid family. *Plasmid* 60:19–37.
- Chai Y, Winans SC. 2005. A small antisense RNA downregulates expression of an essential replicase protein of an *Agrobacterium tumefaciens* Ti plasmid. *Mol. Microbiol.* 56:1574–1585.
- Chen Y, et al. 2010. Complete genome sequence of the aerobic facultative methanotroph *Methylocella silvestris* BL2. *J. Bacteriol.* 192:3840–3841.
- Chevreur B, Wetter T, Suhai S. 1999. Genome sequence assembly using trace signals and additional sequence information, p 45–56. *Computer science and biology: Proceedings of the German Conference on Bioinformatics*. Research Centre for Biotechnology (GBF), Braunschweig, Germany.
- Dam B, Ghosh W, Das Gupta SK. 2009. Conjugative type 4 secretion system of a novel large plasmid from the chemoautotroph *Tetrathiodibacter kashmirensis* and construction of shuttle vectors for *Alcaligenaceae*. *Appl. Environ. Microbiol.* 75:4362–4373.
- Delcher AL, Harmon D, Kasif S, White O, Salzberg SL. 1999. Improved microbial gene identification with GLIMMER. *Nucleic Acids Res.* 27:4636–4641.
- Dunfield PF, et al. 2002. Isolation of a *Methylocystis* strain containing a novel *pmoA*-like gene. *FEMS Microbiol. Ecol.* 41:17–26.
- Gordon D. 2003. Viewing and editing assembled sequences using Consed, chapter 11, unit 11.2. *In Current protocols in bioinformatics*. John Wiley and Sons, Somerset, NJ.
- Hamilton CM, et al. 2000. TraG from RP4 and TraG and VirD4 from Ti plasmids confer relaxosome specificity to the conjugal transfer system of pTiC58. *J. Bacteriol.* 182:1541–1548.
- Hamlett NV, Landale EC, Davis BH, Summers AO. 1992. Roles of the Tn21 *merT*, *merP*, and *merC* gene products in mercury resistance and mercury binding. *J. Bacteriol.* 174:6377–6385.
- Hassani BK, Astier C, Nitschke W, Ouchane S. 2010. CtpA, a copper-translocating P-type ATPase involved in the biogenesis of multiple copper-requiring enzymes. *J. Biol. Chem.* 285:19330–19337.
- Holloway P, McCormick W, Watson RJ, Chan YK. 1996. Identification and analysis of the dissimilatory nitrous oxide reduction genes, *nosRZDFY*, of *Rhizobium meliloti*. *J. Bacteriol.* 178:1505–1514.
- Hou S, et al. 2008. Complete genome sequence of the extremely acidophilic methanotroph isolate V4, *Methylophilum inferorum*, a representative of the bacterial phylum *Verrucomicrobia*. *Biol. Direct* 3:26. doi:10.1186/1745-6150-3-26.
- Lidstrom ME, Stirling DI. 1990. Methylophilus: genetics and commercial applications. *Annu. Rev. Microbiol.* 44:27–58.
- Lidstrom ME, Wopat AE. 1984. Plasmids in methanotrophic bacteria: isolation, characterization and DNA hybridization analysis. *Arch. Microbiol.* 140:27–33.
- Mazur A, Majewska B, Stasiak G, Wielbo J, Skorupska A. 2011. *repABC*-based replication systems of *Rhizobium leguminosarum* bv. *trifolii* TA1 plasmids: incompatibility and evolutionary analyses. *Plasmid* 66:53–66.
- Pandey DP, Gerdes K. 2005. Toxin-antitoxin loci are highly abundant in free-living but lost from host-associated prokaryotes. *Nucleic Acids Res.* 33:966–976.
- Rasko DA, et al. 2007. Complete sequence analysis of novel plasmids from emetic and periodontal *Bacillus cereus* isolates reveals a common evolutionary history among the *B. cereus*-group plasmids, including *Bacillus anthracis* pXO1. *J. Bacteriol.* 189:52–64.
- Richardson D, Felgate H, Watmough N, Thomson A, Baggs E. 2009. Mitigating release of the potent greenhouse gas N₂O from the nitrogen cycle—could enzymic regulation hold the key? *Trends Biotechnol.* 27:388–397.

29. Semrau JD, DiSpirito AA, Yoon S. 2010. Methanotrophs and copper. *FEMS Microbiol. Rev.* **34**:496–531.
30. Smith SM, et al. 2011. Crystal structure and characterization of particulate methane monooxygenase from *Methylocystis* species strain M. *Biochemistry* **50**:10231–10240.
31. Stein LY, et al. 2011. Genome sequence of the methanotrophic alphaproteobacterium *Methylocystis* sp. strain Rockwell (ATCC 49242). *J. Bacteriol.* **193**:2668–2669.
32. Stein LY, Klotz MG. 2011. Nitrifying and denitrifying pathways of methanotrophic bacteria. *Biochem. Soc. Trans.* **39**:1826–1831.
33. Stein LY, et al. 2010. Genome sequence of the obligate methanotroph *Methylosinus trichosporium* strain OB3b. *J. Bacteriol.* **192**:6497–6498.
34. Stolyar S, Costello AM, Peeples TL, Lidstrom ME. 1999. Role of multiple gene copies in particulate methane monooxygenase activity in the methane-oxidizing bacterium *Methylococcus capsulatus* Bath. *Microbiology* **145**:1235–1244.
35. Summers AO. 1986. Organization, expression, and evolution of genes for mercury resistance. *Annu. Rev. Microbiol.* **40**:607–634.
36. Svenning MM, et al. 2011. Genome sequence of the arctic methanotroph *Methylobacter tundripaludum* SV96. *J. Bacteriol.* **193**:6418–6419.
37. Uraji M, Suzuki K, Yoshida K. 2002. A novel plasmid curing method using incompatibility of plant pathogenic Ti plasmids in *Agrobacterium tumefaciens*. *Genes Genet. Syst.* **77**:1–9.
38. Vuilleumier S, et al. 2012. Genome sequence of the haloalkaliphilic methanotrophic bacterium *Methylomicrobium alcaliphilum* 20Z. *J. Bacteriol.* **194**:551–552.
39. Ward N, et al. 2004. Genomic insights into methanotrophy: the complete genome sequence of *Methylococcus capsulatus* (Bath). *PLoS Biol.* **2**:e303. doi:10.1371/journal.pbio.0020303.
40. Warner P, Higgins I, Drozd J. 1977. Examination of obligate and facultative methylotrophs for plasmid DNA. *FEMS Microbiol. Lett.* **1**:339–342.